Received: 3 September 2018 | Revised: 12 November 2018 | Accepted: 20 November 2018

DOI: 10.1002/er.4347

Check for updates

SHORT COMMUNICATION

WILEY INTERNATIONAL JOURNAL OF ENERGY RESEARCH

A coupled and interactive influence of operational parameters for optimizing power output of cleaner energy production systems under uncertain conditions

Dezhi Chen[1] | Surinder Singh[2] | Liang Gao[3] | Akhil Garg[1] | Zhun Fan[4] | Chin-Tsan Wang[5]

[1] Intelligent Manufacturing Key Laboratory of Ministry of Education, Shantou University, Shantou, Guangdong, China

[2] Department of Mechanical Engineering, Indian Institute of Technology, Ropar, India

[3] State Key Lab of Digital Manufacturing Equipment and Technology, School of Mechanical Science and Engineering, Huazhong University of Science and Technology, Wuhan, China

[4] Guangdong Provincial Key Laboratory of Digital Signal and Image Processing, College of Engineering, Shantou University, Shantou 515063, China

[5] Department of Mechanical and Electro-Mechanical Engineering, National I Lan University, ILan, Taiwan

Correspondence
Liang Gao, State Key Laboratory of Digital Manufacturing Equipment and Technology, School of Mechanical Science and Engineering, Huazhong University of Science and Technology, Wuhan, China.
Email: gaoliang@mail.hust.edu.cn Akhil Garg, Intelligent Manufacturing Key Laboratory of Ministry of Education, Shantou University, Shantou, Guangdong, China.
Email: akhil@stu.edu.cn

Funding information
Department of Education of Guangdong Province; Sailing Talent Program, Shantou University Youth Innovation Talent Project, Grant/Award Number: 2016KQNCX053; State Key Lab of Digital Manufacturing Equipment and Technology (Huazhong University of Science and Technology), Grant/Award Number: DMETKF2018019

Summary

The mechanisms in proton-exchange membrane fuel cells (PEMFCs) cannot be explicitly represented by a mathematical function because the PEMFC system is multi-dimensional and complex and represents uncertainty in operation variables, which cannot be modeled by experiments or by trial-and-error approach. Therefore, this work proposes to study the coupled and interactive influence of stack current (SC), stack temperature (ST), oxygen excess ratio (OER), hydrogen excess ratio (HER), and inlet air humidity (IAH) for optimizing the power output of PEMFC. The data obtained from the experiments have been inserted into architecture of automated neural-network search, which automates the selection of error function, activation function, uncertainties in inputs and number of hidden neurons in formulation of a robust and accurate model for power density as a function of five operational variables. Among the operational variables, the correlation coefficient between the SC and the output power is the highest, followed by OER, and the ST. However, for HER and IAH, the power output follows negative nonlinear relation. The optimization converged at 130th iteration results in maximum power output of 3410 W for an optimum value of SC (51A), ST (59°C), OER (3:2), HER (1:10), and IAH (0.8).

KEYWORDS

hydrogen excess ratio, polymer electrolyte membrane fuel cells, power output, stack current, uncertain operational PEMFC variables

 © 2019 John Wiley & Sons, Ltd.

1 | INTRODUCTION

The shortage of the natural resources, such as oil and coal, has become one of the most urgent problems in the world due to increase of usage. Mass consumption of the natural resources has been resulted in global warming. Today, researchers are working towards developing new ways of replacing the use of natural resource. Hydrogen fuel cell has been considered as substitute for fossil fuel for the future, because of its high efficiency and environmental protection characteristics. Advantages of hydrogen fuel cell are zero emission levels, high power output, structural safety, and multiple uses.[1] Among hydrogen fuel cells, the polymer electrolyte membrane fuel cell (PEMFC) is the most promising in virtue of its high power/volume and power/mass densities, safety, and more. Illustration of the main structure and functioning of a PEMFC is shown in Figure 1. The cathode and anode are the two electrodes of the fuel cell. An electrolyte (membrane) has been placed between the two electrodes which allows only the proton to pass through. Two bipolar plates have been included on both sides of the fuel cell, which act as current collectors and flow distributors of O_2 and H_2 (which are the main reactants during the operation of PEMFC). H_2 flows towards the anode and separates into an electron and a proton (H^+) under the chemical action of catalyst (as represented by equation numbers 1 and 2). The H^+ flows through the electrolyte and reacts with O_2 in the cathode side to form water, while releasing energy and generating heat. Whereby the electron flows through an external circuit to produce electricity.[2]

$$2H_2 - 4e^- == 4H \tag{1}$$

$$O_2 + 2e^- + 4H^+ == 2H_2O \tag{2}$$

There are many fields in which the fuel cells have been applied. The automobile industry is one key area. Ballard has developed a few forms of PEM fuel cells which have been used in vehicle production since 2000s.[3] However, the cost of the utilizing PEM fuel cells is high; this requires that the fuel cell should be used as efficiently as possible.[4] Furthermore, the production and storage problem of H_2 should be solved for the operation.[3,5-7] Researches in modeling of PEM fuel cell have begun in 1990s. In the 21st century, researches in furthering the optimization of PEM fuel cells are still ongoing and the effect of uncontrollable factors on output power should be addressed first. In different researches, operating parameters, viz, temperature, pressure, and current density, have been usually thought to be the main factors that influence the output power of PEMFC.[8-11] Recently, a research has used a new methodology: moment-based uncertainty evaluation technique, a framework which is accurate and reliable to study the influence of some uncontrollable factors, viz, SC, stack temperature (ST), oxygen excess ratio (OER), inlet air humidity (IAH), and hydrogen excess ratio (HER).[3,12-22] To some extent, these uncontrollable factors have a bad influence on the output power and operation of the fuel cell.[2] However, the relation between the output power and these parameters cannot be explicitly represented by a mathematical function, because the PEMFC system is multi-dimensional and complex, which cannot be modeled by experiments or by trial-and-error approach.

Therefore, this work proposes to study the coupled and interactive influence of SC, ST, OER, HER, and IAH for optimizing the power output of PEMFC. The data obtained from experiments have been inserted into architecture of automated neural-network search (ANS), which automates the selection of error function, activation function, uncertainties in inputs, and number of hidden neurons in formulation of a robust and accurate model for power density as a function of five operational variables. 2-D and 3-D surface plots are then shown to illustrate the individual and interactive relationships between the power output and five operational parameters. Simulation design profile is obtained to illustrate the robustness of the formulated model for parameters beyond the given input range. In the last, the optimization is performed on the

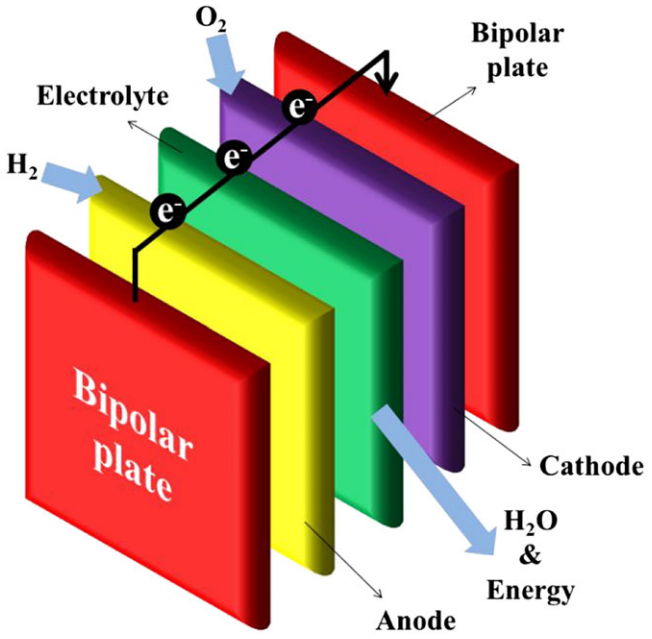

FIGURE 1 Illustration of the main structure and functioning of polymer electrolyte membrane (PEM) fuel cell [Colour figure can be viewed at wileyonlinelibrary.com]

power output of PEMFC for obtaining the optimum values of five operational parameters.

2 | RESEARCH PROBLEM

In the experiments, the hydrogen mass flow rate was set as an input parameter and the output power was set as an output parameter. Consequently, these experiments have shown that the hydrogen mass flow rate was at a low level when the output power was maximum.[5] The mass flow rate of hydrogen can be related to the output power by Equation 3.

$$WH_2 = MH_2 n \lambda_{an} \quad (3)$$

WH_2 denotes hydrogen mass flow rate, λ_{an} indicates the hydrogen stoichiometric ratio, 1st indicates the SC, F indicates the Faraday constant, MH_2 indicates the hydrogen molecular mass, and n indicates the cell numbers. On the other hand, the PEMFC output power was considered as a function of different operational parameters like: SC, ST, OER, HER, and IAH. These five parameters were the main factors that influence the output power of a PEMFC. Some researchers have found the influence of each parameter on the output power. The air was used as reactant and coolant in the operation of PEMFC to limit the output power. The increase of operating temperature increased the reaction speed, which led to a higher output power.[23] However, higher operating temperature led to the diminishment of the catalyst dispersion and the electrochemical surface of the catalysts and also the membrane lifetime issues and failure.[24] In that case, the operating temperature should be controlled at an appropriate range.[25] With the increase of current density, the oxygen and hydrogen consumption will be increased which leads to the increase of reactants mass flow rates.[26,27] During the operation of PEM fuel cell, ohmic losses were a main factor that leads to the diminishment of the output power. Humidity was an important parameter to decrease the membrane electrical resistance and therefore the ohmic losses, so an appropriate range of

TABLE 1 Ten ANS models as per their training and testing performances

Model	Net. Name	Training Pref.	Testing Pref.	Validation Pref.
1	MLP 5-8-1	0.996393	0.960111	0.999356
2	MLP 5-6-1	0.998248	0.971375	0.999117
3	MLP 5-4-1	0.998155	0.983045	0.999775
4	MLP 5-3-1	0.996994	0.974117	0.999283
5	MLP 5-7-1	1.000000	0.998225	0.999796
6	MLP 5-8-1	0.993665	0.981217	0.999692
7	**MLP 5-7-1**	**0.999993**	**0.999872**	**0.999625**
8	MLP 5-6-1	0.996660	0.983334	0.999848
9	MLP 5-6-1	0.999561	0.999057	0.999138
10	MLP 5-4-1	0.997848	0.978292	0.999073

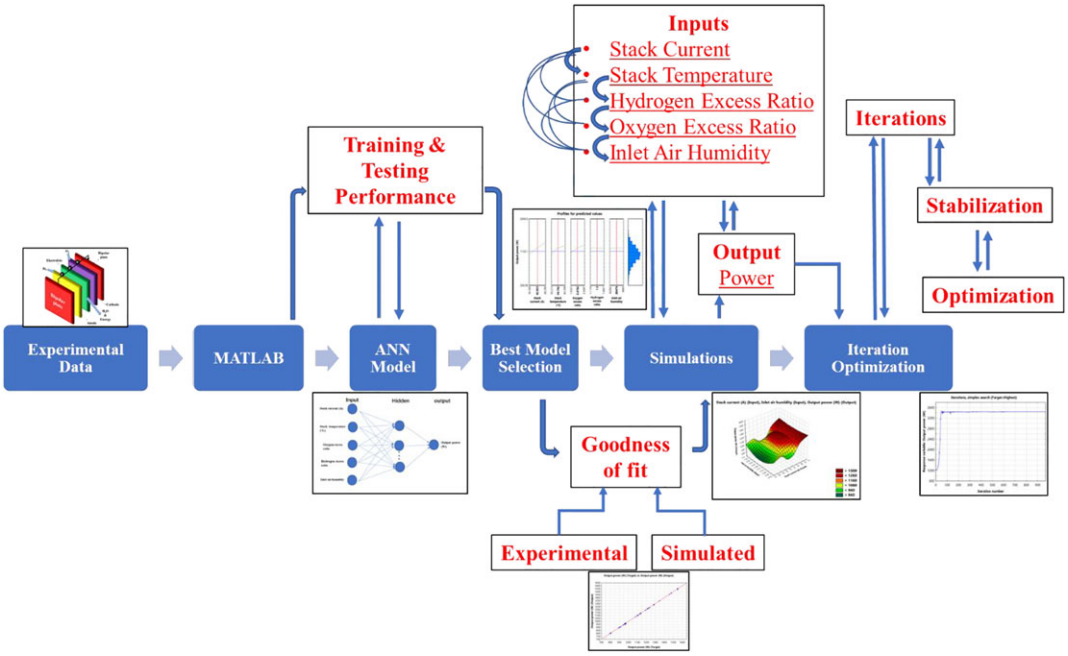

FIGURE 2 Schematic of proposed methodology to investigate the effect of uncontrollable parameters on the power of PEMFC [Colour figure can be viewed at wileyonlinelibrary.com]

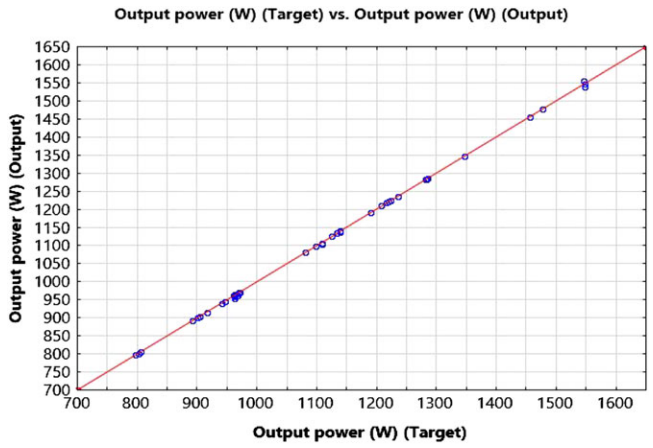

FIGURE 3 Goodness of fit for experimental vs simulated results of the selected ANS model [Colour figure can be viewed at wileyonlinelibrary.com]

humidity was required during the operation of PEM fuel cell.[28] Therefore, PEMFC power output is a function of five operational parameters such as SC, ST, OER, HER, and IAH. However, the mechanism and the relation in-between the output power and input parameters cannot be explicitly represented by a mathematical function because the PEMFC system is multi-dimensional and complex and represents uncertainty in operation variables, which cannot be modeled by experiments or by trial-and-error approach. The present work performs study of coupled and interactive influence of SC, ST, OER, HER, and IAH for optimizing the power output of PEMFC.

3 | PROPOSED ANS

The schematic of proposed methodology to study the effect of uncontrollable parameters on the power output of PEMFC is shown in Figure 2.

3.1 | Automated neural network search (ANS)

Automated neural-network search approach is powerful variation of artificial neural networks (ANN), where the uncertainties in the selection of activation function, error function, uncertainties in inputs, and number of hidden neurons are done automatically. A computational model created by Warren McCulloch and Walter Pitts[29] for neural networks (according to mathematics and algorithms, called threshold logic) has been used. The network depends on the complications of the system to attain the purpose of dealing out information by regulating the weight of the interconnections among the large number of nodes (neurons) inside. Each node in ANS represents a specific function called activation function. The networks consisted of three layers, viz, the input layer, the hidden layer comprising certain number of neurons, and the output layer. Input consists of five parameters, viz, SC, ST, OER, HER, and IAH, while the only output parameter is the power of fuel cell. Although those parameters are not directly related or nonlinear with the output power, the neural network is very good at searching an obscure relationship between them. The definition of weight is the connection between two nodes, each representing a weighted value of the

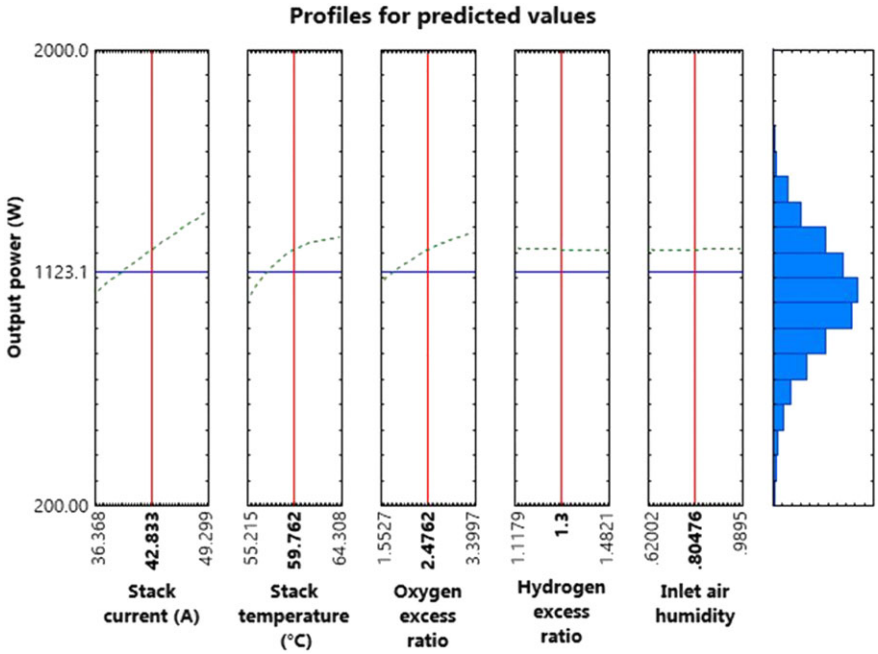

FIGURE 4 Profiles for simulation results of predicted values of the power output of the selected ANN model under permissible conditions [Colour figure can be viewed at wileyonlinelibrary.com]

connection signal. The weights and the functions used to compute the activation can be modified by a learning process which is governed by a learning rule. ANS is trained by learning to obtain the network weight and structure and shows a strong self-learning ability and adaptivity.

3.2 | Parameter settings of ANS

During the training process, multiple preliminary tests are implemented to change the parameter value to improve the accuracy of the results. Seventy percent of the data has been used for training purpose, and 30% of the data has been divided in two halves (15% for validation and 15% for testing of the ANS model). Since the maximum hidden units must not exceed the number of training data for radial basis function networks,[30] the maximum hidden units of radial basis function networks have been set as 11 accordingly.

Table 1 shows the training performance and testing performance of the models with various network settings. Among 10 models, the model No.7 (MLP 5-7-1) with the best performance according to training and testing performances is selected for further analysis (bolded and underlined). Figure 3 represents the goodness of fit performance of the selected ANS model. The target represents the actual value obtained from the experimental data, and the output values are obtained from the estimated value of the ANS model. A complete matching of all data points (of experimental line and simulated) on fitness line can be observed in Figure 3. It shows that the expected result simulated by ANS model is almost the same as the original

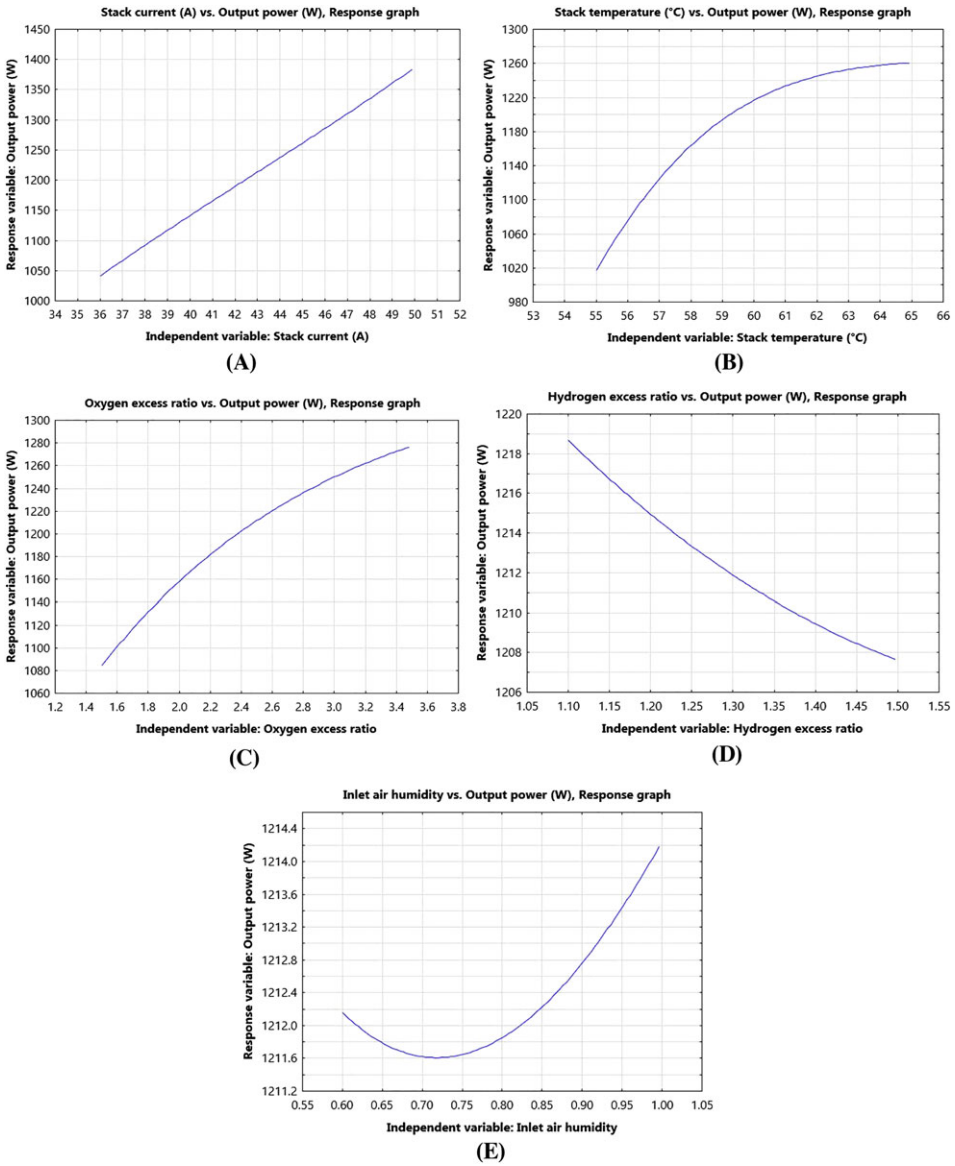

FIGURE 5 2-D graphs illustrating the response of (A) stack current, (B) stack temperature, (C) oxygen excess ratio, (D) hydrogen excess ratio, and (E) inlet air humidity, to the output in the ANS model [Colour figure can be viewed at wileyonlinelibrary.com]

data, which depicts the high degree of accuracy of the selected ANS model (model No.7 [MLP 5-7-1]).

Simulation results of the power output of the selected model under permissible conditions are illustrated in Figure 4. By individually observing the effects of each input parameters, it can be stated that, with increase in input stack current (SC), output power density has been increased linearly. Similarly, with increase in ST, power density has been increased but became constant after certain value. Oxygen excess ratio showed almost the linear relation with power density of fuel cell. However, HER and air humidity showed almost negligible effect of the power density of the PEMFC. For observing the combined effect of these input parameters on power density, it was

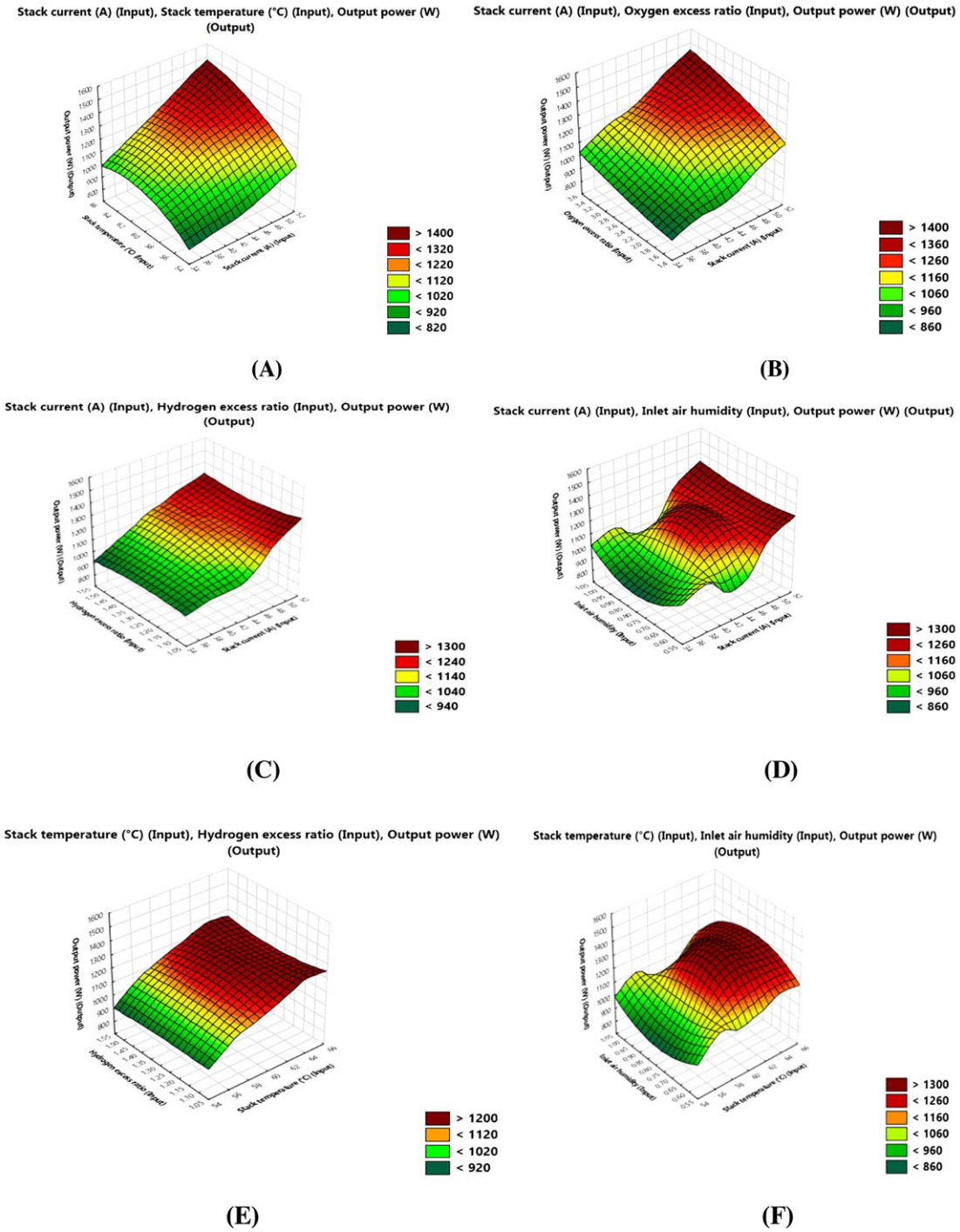

FIGURE 6 Interaction simulations of (A) SC and ST; (B) SC and OER; (C) SC and HER; (D) SC and IAH; (E) ST and HER; (F) ST and IAH; (G) ST and OER; (H) OER and HER; (I) OER and IAH; and (J) HER and IAH, with the output power of the PEMFC [Colour figure can be viewed at wileyonlinelibrary.com]

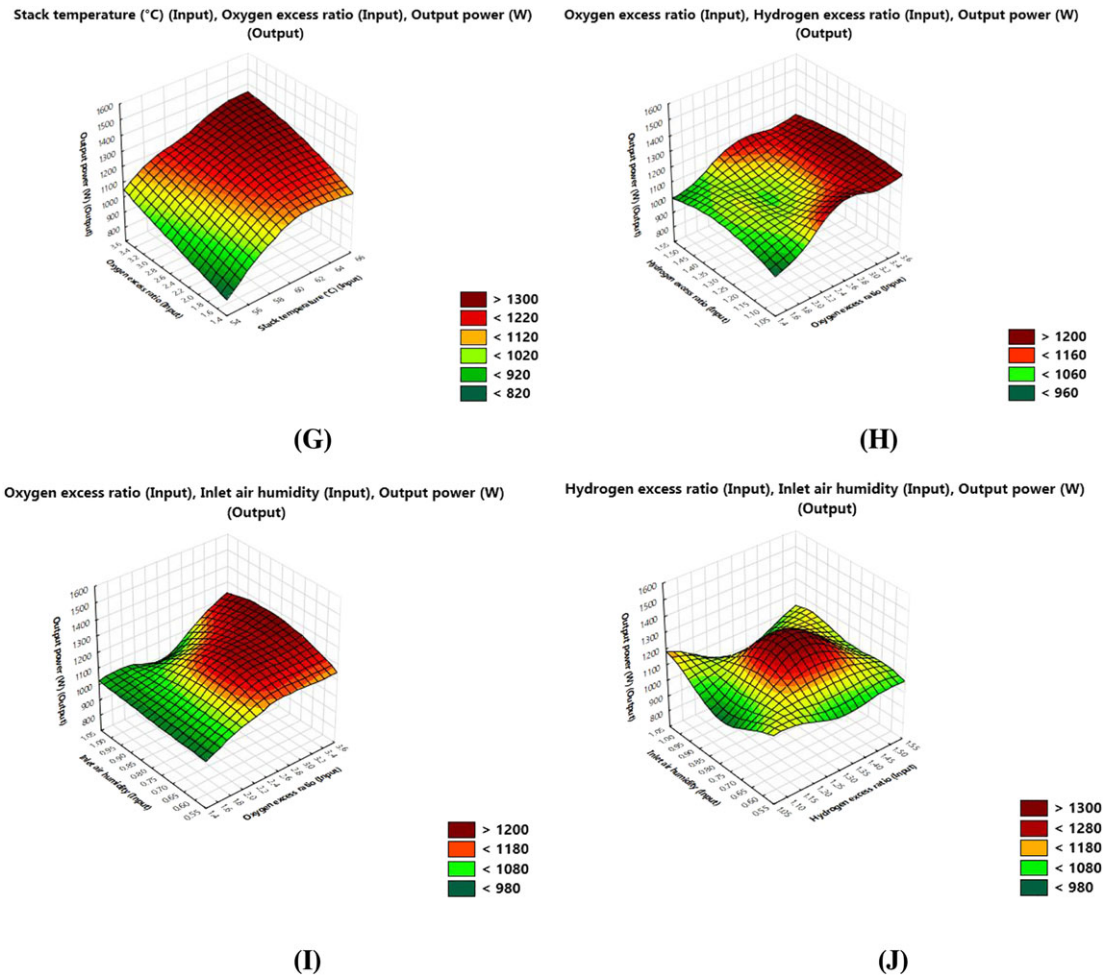

FIGURE 6 Continued.

assumed that all the five inputs follow the normal distribution. Their minimum and maximum values are shown in Figure 4. It is observed that, in the range of 200 to 2000 W, output power simulated by the model follows an approximate normal distribution. Therefore, it can be revealed that even when the data are outside the given input range, the simulation results will show similarity with the actual results. This validates the robustness of model for both interpolation and extrapolation cases.

To further investigate the response of single operational variable on the power output of PEMFC obtained from ANS model, 2-D surface plots are illustrated in Figure 5. Figure 5 shows the extent to which the single variable affects the output when averaging the rest of the variables. Figure 5A,B,C shows that the three variables, vz, SC, ST, and OER, are positively correlated with the output power. Among them, the correlation coefficient between the SC and the output power is the highest, followed by OER, and the ST. Figure 5D shows a strong negative correlation between the HER and the output power. Figure 5E shows that when the IAH is less than 0.72, it is negatively related to the output power, but when IAH is greater than 0.72, it is positively correlated with the output power.

For studying the interaction between combination of two input variables, 3-D surface plots have been represented in Figure 6. Figure 6A,B,C,D shows the 3-D graphs showing the correlation between SC and ST; SC and OER; SC and HER; and SC and IAH, respectively, with respect to output power. It has been observed that the interactions between the SC and the ST, SC, and OER, and SC and HER, are small, and they all are positively correlated with the output power. The interaction between SC and IAH on output power is larger. When the value of the SC is between 34 and 40 A, the output power first decreases with the increase of inlet air flow rate and then increases. When the SC exceeded 46 A, IAH has little effect on the output power. The interaction of ST and HER, ST and IAH, and ST and OER, with output power of PEMFC, has been represented in Figure 6E,F,G respectably. It has been observed that the interactions between the ST with HER, and ST with OER, are small to the output power, and they all are positively correlated with the output power. The interaction between ST with IAH on output power is larger. When

the value of the ST is between 54°C and 60°C, the output power first decreases with the increase of inlet air flow rate and then increases. When the ST exceeded 60°C, IAH has little effect on the output power. Similarly, the interaction among OER and HER, OER and IAH, and HER and IAH with the output power of the PEMFC has been represented in Figure 6H,I,J, respectably. It has been observed that the interaction relationship between the two sets of variables (viz, OER and HER, OER and IAH) is small (Figure 6H,I). When the two variables have been changed, the change of the output power is small. However, when the value of HER is 1.20 to 1.45, the output power increases first and then decreases with the increase of IAH (Figure 6J). When the value of IAH is increased from 0.63 to 092, the output power increases, and it is decreased with further increase in HER. The two variables show a greater impact on the value of the output power. The maximum output power has been obtained when the value of the HER is 1.31 and the value of the IAH is 0.78.

By observing the overall interactions of all five input factors, it has been observed that, when the interaction between the two variables is small, the curved surface trend of the 3D graph is closer to the superposition of their response graph. But, if the interaction between the two variables is large, the curved surface trend of the 3D graph would be different from the overlay of their response graph. Further, for maximizing the power output from PEMFC, NSGA II combined with iterative and search algorithm is used. The model parameters have been modified (iterations have been made) many times, so that the results of the model get approximated to the maximum output expected. The optimization converged at 130th iteration results in maximum power output of 3410 W for an optimum value of SC (51A), ST (59°C), OER (3.2), HER (1.10), and IAH (0.8).

4 | CONCLUSIONS

The present work undertakes research problem on study of coupled and interactive influence of five operational parameters for optimizing the power output of PEMFC under uncertain operational variables conditions. In this context, the present work proposes an ANS approach. From the results and discussions, the following conclusions have been drawn:

1. The correlation coefficient between the SC and the output power is the highest, followed by OER, and the ST.
2. A strong negative correlation between the HER and the output power, but, IAH is positively correlated with the output power.
3. Output power simulated by the model follows an approximate normal distribution. Therefore, it can be revealed that even when the data are outside the given input range, the simulation results will show similarity with the actual results. This validates the robustness of model for both interpolation and extrapolation cases.
4. When the interaction between the two variables is small, the curved surface trend of the 3D graph is closer to the superposition of their response graph. But, if the interaction between the two variables is large, the curved surface trend of the 3D graph would be different from the overlay of their response graph.
5. The optimization converged at 130th iteration results in maximum power output of 3410 W for an optimum value of SC (51A), ST (59°C), OER (3.2), HER (1.10), and IAH (0.8).

Therefore, from above all the points, it can be depicted that the reliability of the proposed ANS model is high and can be used efficiently to investigate the effect of unfavorable factors on the output power of PEMFCs. Future work shall consider the hybridization of ANN with finite element simulation[31] and uncertainty analysis for real-time diagnosis of fuel cell.[32-34]

ACKNOWLEDGEMENTS

Authors acknowledge Grant DMETKF2018019 by State Key Lab of Digital Manufacturing Equipment and Technology (Huazhong University of Science and Technology). Authors also like to acknowledge the Sailing Talent Program, Shantou University Youth Innovation Talent Project (2016KQNCX053) supported by the Department of Education of Guangdong Province.

CONFLICT OF INTEREST

None.

ORCID

Dezhi Chen https://orcid.org/0000-0003-3291-0693
Surinder Singh https://orcid.org/0000-0002-3375-6088
Liang Gao https://orcid.org/0000-0002-1485-0722
Akhil Garg https://orcid.org/0000-0001-5731-4105
Chin-Tsan Wang https://orcid.org/0000-0003-0989-076X

REFERENCES

1. Özgür T, Yakaryılmaz AC. A review: exergy analysis of PEM and PEM fuel cell based CHP systems. *Int J Hydrogen Energy*. 2018;43(38):17993-18000.

2. Ellis MW, Von Spakovsky MR, Nelson DJ. Fuel cell systems: Efficient, flexible energy conversion for the 21st century. *Proceedings of the IEEE*. 2001;89(12):1808-1818.

3. Garg A, Shankhwar K, Jiang D, Vijayaraghavan V, Panda BN, Panda SS. An evolutionary framework in modelling of multi-output characteristics of the bone drilling process. *Neural Comput Applic*. 2018;29(11):1233-1241.
4. Taner T. Energy and exergy analyze of PEM fuel cell: a case study of modeling and simulations. *Energy*. 2018;143:284-294.
5. Rajan A, Garg A, Vijayaraghavan V, Ye CK, Ooi PL. Parameter optimization of polymer electrolyte membrane fuel cell using moment-based uncertainty evaluation technique. *J Energy Storage*. 2018;15:8-16.
6. Trinke P, Bensmann B, Hanke-Rauschenbach R. Current density effect on hydrogen permeation in PEM water electrolyzers. *Int J Hydrogen Energy*. 2017;42(21):14355-14366.
7. Fallisch A, Schellhase L, Fresko J, et al. Investigation on PEM water electrolysis cell design and components for a HyCon solar hydrogen generator. *Int J Hydrogen Energy*. 2017;42(19):13544-13553.
8. Myers RH, Montgomery DC. Response surface methodology: process and product in optimization using designed experiments. *J Statist Plann Inference*. 1997;38(3):284-286.
9. Mohamed W, Kamil M. Hydrogen preheating through waste heat recovery of an open-cathode PEM fuel cell leading to power output improvement. *Energ Conver Manage*. 2016;124:543-555.
10. Mckamey, C. G., & Maziasz, P. J. (1994). Effect of heat treatment temperature on creep-rupture properties of FeâAl-based alloys.
11. Asghari S, Mokmeli A, Samavati M. Study of PEM fuel cell performance by electrochemical impedance spectroscopy. *Int J Hydrogen Energy*. Sep. 2010;35(17):9283-9290.
12. Waller MG, Walluk MR, Trabold TA. Performance of high temperature PEM fuel cell materials. Part 1: effects of temperature, pressure and anode dilution. *Int J Hydrogen Energy*. 2016;41(4):2944-2954.
13. Blunier, B. "Air management in PEM fuel cells: state-of-the-art and prospectives," p. 10.
14. Cruz Rojas A, Lopez Lopez G, Gomez-Aguilar J, Alvarado V, Sandoval Torres C. Control of the air supply subsystem in a PEMFC with balance of plant simulation. *Sustainability*. Jan. 2017;9(1):73.
15. Feroldi D, Basualdo M. Description of PEM fuel cells system. In: Basualdo MS, Feroldi D, Outbib R, eds. *PEM Fuel Cells with Bio-Ethanol Processor Systems*. London: Springer London; 2012:49-72.
16. Cieslinski, J. T. Kaczmarczyk, T. and Dawidowicz, B. "Performance of the PEM fuel cell module. Part 2. Effect of excess ratio and stack temperature," p. 6, 2017.
17. Vasu G. and Tangirala, A. Control of air flow rate with stack voltage measurement for a PEM fuel cell system. 2018.
18. Xuan D, Li Z, Kim J, Kim Y. Optimal operating points of PEM fuel cell model with RSM. *J Mech Sci Technol*. Mar. 2009;23(3):717-728.
19. Grujicic, M. Chittajallu, K. M. and Pukrushpan, J. T. "Control of the transient behaviour of polymer electrolyte membrane fuel cell systems," vol. 218, p. 12, 2004.
20. Qin C, Wang J, Yang D, Li B, Zhang C. Proton exchange membrane fuel cell reversal: a review. *Catalysts*. Dec. 2016;6(12):197.
21. Pukrushpan, J. T. Stefanopoulou, A. G. and Peng, H. "Modeling and control for PEN fuel cell stack system," p. 6.
22. Pukrushpan JT, Peng H, Stefanopoulou AG. Control-oriented modeling and analysis for automotive fuel cell systems. *J Dyn Syst Meas Control*. 2004;126(1):14.
23. Trinke P, Bensmann B, Hanke-Rauschenbach R. Experimental evidence of increasing oxygen crossover with increasing current density during PEM water electrolysis. *Electrochem Commun*. 2017;82:98-102.
24. Grigoriev SA, Millet P, Volobuev SA, Fateev VN. Optimization of porous current collectors for PEM water electrolysers. *Int J Hydrogen Energy*. 2009;34(11):4968-4973.
25. Misran E, Hassan NSM, Wan RWD, Majlan EH, Rosli MI. Water transport characteristics of a PEM fuel cell at various operating pressures and temperatures. *Int J Hydrogen Energy*. 2013;38(22):9401-9408.
26. Rao SSL, Shaija A, Jayaraj S. Performance analysis of a transparent PEM fuel cell at the optimized clamping pressure applied on its bolts. *Mater Today Proc*. 2018;5(1):58-65.
27. Zhao D, Xu L, Huangfu Y, Dou M, Liu J. Semi-physical modeling and control of a centrifugal compressor for the air feeding of a PEM fuel cell. *Energ Conver Manage*. 2017;154:380-386.
28. Ashrafi M, Shams M. The effects of flow-field orientation on water management in PEM fuel cells with serpentine channels. *Appl Energy*. 2017;208:1083-1096.
29. McCulloch W, Pitts W. A logical calculus of ideas immanent in nervous activity. *Bull Math Biophys*. 1943;5(4):115-133. https://doi.org/10.1007/BF02478259
30. Broomhead DS, Lowe D. Multivariate functional interpolation and adaptive network. *Complex Syst*. 1988;2:321-355.
31. Vijayaraghavan V, Zhang L. Effective mechanical properties and thickness determination of boron nitride nanosheets using molecular dynamics simulation. *Nanomaterials*. 2018;8(7):546.
32. Zhou WH, Tan F, Yuen KV. Model updating and uncertainty analysis for creep behavior of soft soil. *Comput Geotech*. 2018;100(2018):135-143.
33. Tan F, Zhou WH, Yuen KV. Effect of loading duration on uncertainty in creep analysis of clay. *Int J Numer Anal Methods Geomech*. 2018;42:1235-1254.
34. Gamse S, Zhou WH, Tan F, Yuen KV, Oberguggenberger M. Hydrostatic-season-time model updating using Bayesian model class selection. *Reliab Eng Syst Saf*. 2018;169(2018):40-50. https://doi.org/10.1016/j.ress.2017.07.018

How to cite this article: Chen D, Singh S, Gao L, Garg A, Fan Z, Wang C-T. A coupled and interactive influence of operational parameters for optimizing power output of cleaner energy production systems under uncertain conditions. *Int J Energy Res*. 2019;1–9. https://doi.org/10.1002/er.4347